Title
GRAIN REFINEMENT THROUGH THERMAL CYCLING IN AN Fe-Ni-Ti CRYOGENIC ALLOY

Authors
Jin, S.
Morris, W.
Zackay, V.F.

Publication Date
1973-12-01

Submitted to Metallurgical Transactions

LBL-2539
Preprint

GRAIN REFINEMENT THROUGH THERMAL CYCLING IN AN Fe-Ni-Ti CRYOGENIC ALLOY

S. Jin, J. W. Morris, Jr. and V. F. Zackay

December 1973

Prepared for the U.S. Atomic Energy Commission under Contract W-7405-ENG-48

DISCLAIMER

GRAIN REFINEMENT THROUGH THERMAL CYCLING IN AN Fe-Ni-Ti CRYOGENIC ALLOY

S. Jin, J. W. Morris, Jr. and V. F. Zackay
Department of Materials Science and Engineering,
University of California and Center for the Design of Alloys,
Inorganic Materials Research Division, Lawrence Berkeley Laboratory,
Berkeley, California 94720

ABSTRACT

A thermal cycling technique which allows the grain refinement of Fe-12Ni-0.25Ti alloy from 40∿60 μm (ASTM #5∿6) to 0.5 ~ 2 μm (ASTM #15∿18) in four cycles has been developed. The process consists of alternate annealing in γ range and (α + γ) range with intermediate air cooling. The transformation behavior, the change of microstructures and cryogenic mechanical properties on each cycling step are described.

Due to the ultrafine grain size, the ductile-brittle transition temperature of this ferritic alloy in Charpy impact testing was suppressed below 6°K. In fracture toughness testing at 77°K, the mode of fracture was altered from brittle quasi-cleavage to complete ductile rupture through the grain refining.

INTRODUCTION

Recent research in this laboratory[1-4] has shown that alloys from the Fe-Ni-Ti system (e.g., Fe-12Ni-0.25Ti) can be processed to have a promising combination of strength and toughness at cryogenic temperature. As expected, the ductile-brittle transition temperatures of these alloys tend to decrease if the effective grain size is made small. Hence a major focus of our research has been on the design of processes which accomplish significant grain refinement.

Previous work[5-7] established two techniques for refining the grain size of Fe-Ni alloys of moderate nickel content. Following studies by Grange[8], Porter and Dabkowski[5] demonstrated grain refinement through a thermal cycling procedure which included repeated cycles of rapid austenitizing and cooling. Grain size as small as 3-5μm (mean intercept length: ASTM #13-14) was obtained. Saul et al[6] also observed grain refinement in maraging steels on simple repeated austenitizing (from ASTM #2 to #7 in 4 cycles). An alternate technique was used by Miller[7], who reported ultrafine grain size (0.3-1.1 μm; ASTM #17-19) in an Fe-Ni alloy which had been severely cold-worked and then annealed in the two-phase ($\alpha + \gamma$) range.

Variants of both these processing techniques were used in our research[2] on the alloy Fe-12Ni-0.25Ti, and both led to alloys of exceptional strength and ductility at cryogenic temperature. However, both processing techniques had undesirable features. When the cyclic austenitizing process was used, the grain size seemed to stabilize at 5-10 μm. A further improvement in low temperature ductility might be obtainable with finer grain size. A more refined structure can be achieved with

mechanical working, but mechanical working is often an impractical or undesirable step in final alloy processing. We therefore sought an alternate thermal treatment which would accomplish a grain refinement comparable to that obtainable with mechanical work.

An initial solution to this problem was reported in Ref. 2, where we showed that an Fe-12Ni-0.25Ti alloy could be processed to a grain size near 1.0 μm by treating it with alternate anneals in the austenite (γ) and the two-phase ($\alpha + \gamma$) fields. The resulting alloys showed exceptional ductility in fracture toughness tests at liquid nitrogen temperature ($77^{o}K$). The processing sequence used was, however, complex, involving nine separate annealing steps. We have since found that this processing sequence can be simplified considerably without sacrificing the grain refinement or the low temperature ductility of the resulting alloys. The grain refinement techniques and associated changes in low temperature mechanical properties are described in the following sections.

I. TECHNICAL APPROACH

The technical approach leading to the grain refinement processes used here and in Ref. 2 may be briefly described as follows: The Fe-12Ni-0.25Ti alloy is expected to show roughly the same transformation behavior as the Fe-12Ni binary, given the small amount of Ti present and its partial consumption in scavenging interstitials. Previous research on the transformation behavior of Fe-Ni alloys in this composition range (summarized, for example, by Floreen[9]) indicates that when the alloys are rapidly heated or cooled between room temperature and the γ-field both the $\alpha \rightarrow \gamma$ and the $\gamma \rightarrow \alpha$ transformations occur primarily through a

diffusionless shear mechanism, while if the alloys are annealed within the two phase ($\alpha + \gamma$) field the transformation proceeds through a diffusional nucleation and growth process leading to an equilibrium partitioning of nickel between the two phases. Either transformation mechanism may be used for grain refinement. If α is heated to the γ-field and then cooled to room temperature, a decrease in apparent grain size (or martensite packet size) results, presumably to relieve the internal strain built up during the shear transformation[6]. If α is annealed inside the two phase region a very fine lath-like structure results, presumably from preferential γ nucleation in the boundaries of the martensite plates.[7]

The fine lath-like structure obtained after two-phase anneal is, however, not a desirable structure for high toughness, and may even cause a decrease in toughness due to easy crack propagation parallel to the laths. In Miller's research[7] the stored energy of prior cold work seemed effective in destroying the preferential alignment of those laths. It seems plausible that residual strain from a cyclic shear transformation may accomplish the same effect, particularly if the strain is allowed to accumulate through repeated cycling.

We have, therefore, investigated thermal cycling treatments of the type illustrated schematically in Fig. 1 (the Fe-Ni equilibrium phase diagram was obtained from Hansen[10]) in which austenite reversions are alternated with two-phase decompositions. The annealing temperatures were chosen from the results of dilatometric studies of the kinetics of the phase transformations, with the guiding principal that the austenitizing temperature should be low, to minimize grain growth, while the

two-phase decomposition temperature should be high, to maximize the rate of decomposition. The annealing times and total number of cycles were chosen from metallographic studies of grain refinement and low-temperature mechanical tests of the resulting alloys.

II. MATERIALS AND PROCESS OF GRAIN REFINEMENT

a. Materials Preparation

A low carbon alloy of nominal composition Fe-12Ni-0.25Ti was obtained from pure starting materials (99.9% purity) by induction melting in an inert gas atmosphere. Two twenty pound ingots of 2.75 in. (7.0 cm) diameter were prepared by slow casting in a rotating copper chill mold. Ingot composition was determined to be (in weight percent): 12.07 Ni, 0.26 Ti, 0.001 C, 0.014 N, 0.003 P, 0.004 S, with the balance Fe. The ingots were homogenized under vacuum at 1050°C for 120 hours, cross-forged at ∿1100°C to thick plates 4" (10.2 cm) wide by 0.75" (1.9 cm) thick, then air-cooled to room temperature. The plates were then annealed at 900°C for two hours to remove most of the prior deformation strain and air cooled to room temperature. This final anneal was included to establish a standard initial state for research purposes; our prior work has shown that the processed alloys have somewhat better cryogenic mechanical properties when grain refined directly from the as-forged condition.

b. Phase Transformation Studies

Dilatometric studies were conducted to determine phase transformation kinetics in this alloy. Tube-shaped dilatometry specimens 1.5" (3.8 cm) long and 0.25" (0.64 cm) in diameter with 0.04" (0.1 cm) wall thickness were machined from the annealed starting material. Temperatures

were monitored with a chromel-alumel thermocouple, spot welded at the mid-point of the specimen length. The experiments were carried out with heating and cooling rates of approximately 15°C/min., roughly duplicating the rates used in heat treatment of the alloy.

Sample dilatometric curves are given in Fig. 2. Fig. 2(a) illustrates transformation behavior when an α (martensite) is continuously heated into the γ region, then cooled to room temperature. Reversion to austenite begins at a temperature slightly below the maximum in the dilation curve at 673°C (which we have taken as a measure of the austenite start temperature, A_s) and is completed at a temperature slightly above the minimum in the curve at 715°C (which measures the austenite finish temperature, A_f). On cooling, the martensite transformation begins near 473°C (M_s) and is largely complete by 412°C (M_f). On cycling, the sample undergoes a small permanent set, measured by the offet in the cooling curve at low-temperature. This offset results from transformation strain of the sample and does not signify the presence of retained austenite; no austenite is detected in x-ray studies of samples cycled back to room temperature. Fig. 2 (a) suggests an austenitizing temperature of about 730°C to insure that the transformation is completed, and a maximum two-phase decomposition temperature of about 650°C to insure that shear reversion has not become significant.

Dilatometric curves monitoring isothermal decomposition at 650°C are shown in Fig. 2 (b). The M_s temperature is essentially independent of transformation time ($t \gtrsim 30$ min.) indicating that the nickel content of the γ formed is essentially independent of the γ volume fraction. This γ apparently transforms completely to α on cooling; no retained austenite

is detected in x-ray diffraction analyses of samples cooled to room temperature. (We do, however, find retained austenite after decomposition at temperatures < 600°C).

Given the curves in Fig. 2(b) we can phrase a rough estimate of the rate of decomposition which is useful in selecting an annealing time. If we assume that the dilation is a linear function of the fraction transformed and estimate the dilation on complete transformation from the total offset in the curves of Fig. 2(a), we obtain the estimated isothermal transformation curve shown in Fig. 3. This curve has an asymptote indicating equilibrium with slightly more than 80% γ, which agrees roughly with an estimate based on the Fe-Ni binary phase diagram. We infer from Fig. 3 that an annealing time of 2 hours at 650°C will yield a product which is roughly 60% γ, providing an overall grain refinement near the optimum. This estimate is supported by the metallographic results given below.

If the 730°C/650°C cycle is repeated after decomposition at 650°C, the kinetics of transformation are complicated by the inhomogeneous distribution of nickel through the microstructure. A sample annealed for two hours at 650°C will consist of roughly 60% γ of composition $\sim$13% Ni (estimated from the Fe-Ni binary phase diagram) together with $\sim$40% residual α of mean nickel concentration near 10% (well above the equilibrium at $\sim$4% Ni) which may be heterogeneously distributed. If the material is air cooled to room temperature and then reheated to 730°C regions of different Ni concentration will transform at different temperatures (and perhaps by different mechanisms) leading to the more

complex transformation behavior illustrated by the dilatometer trace shown in Fig. 4. It nonetheless appears that the pronounced shear reversion is essentially complete at 730°C.

Transformation behavior on subsequent cooling depends on the extent of homogenization at 730°C, and hence on the time of anneal, as illustrated by curves (b) and (c) of Fig. 4. An anneal of 2 hours at 730°C is not sufficient to homogenize the alloy. The continued presence of regions of relatively high Ni concentration is indicated by the suppression of the A_s temperature on reheating (curve (d) of Fig. 4). However, after the second 2 hour anneal at 730°C the A_s temperature in the next heating lies above 650°C, indicating that shear reversion to γ does not become pronounced until the temperature is raised above 650°C.

c. Microstructural Changes on Cycling

On the basis of dilatometric and microstructural studies we selected a grain refining process consisting of alternate two-hour anneals at 730°C and 650°C. A four-cycle process is shown schematically in Fig. 1, where the successive steps are labelled 1A (730°C), 1B (650°C), 2A (730°C) and 2B (650°C). The evolution of the microstructure during this cycling is illustrated by the optical micrographs given in Fig. 5 and by the scanning electron micrographs in Fig. 6. After final cycle 2B the bulk of the microstructure consists of a fine mixture of platelet grains approximately 1-4 microns long and a fraction of a micron in the short dimension. The preferential orientation of these grains has been largely eliminated.

A precise characterization of the microstructures developed during this thermal cycling depends on the results of transmission electron

microscopy studies now in progress. The general features of the grain refinement process are, however, apparent in Fig. 5 and Fig. 6. Fig. 5(a) shows the microstructure of the annealed starting material. The apparent grain size is 40-60 μm (ASTM #5-6). After cycle 1A the apparent grain size (Fig. 5(b)) has reduced to ∿15 μm (ASTM #9). These grains consist of blocky laths of dislocated martensite. During cycle 1B the martensite is isothermally decomposed to give the microstructure shown in Fig. 5(c) and in Fig. 6(a) and (b). From the microstructure it appears that the austenite transformation begins along prior austenite grain boundaries, and the austenite then grows into the grains along what appear to be the prior martensite platelet boundaries. After two hours the microstructure consists of a fine admixture of α with γ as platelets or lath shaped particles within grains, and with γ in a more blocky form along the prior grain boundaries. The γ then transforms to α on cooling to room temperature.

The microstructure after cycle 1B is not a desirable one for low temperature toughness. The strong preferential orientation of the microstructural features provides potential paths for easy crack propagation. This preferential orientation is largely removed during the second $730^{\circ}C/650^{\circ}C$ cyclic treatment.

The microstructure after cycle 2A is shown in Fig. 5 (d) and Fig. 6 (c), (d). The evident microstructural changes are two. First, a reaction which we assume to be an homogenization reaction initiates along lath packet boundaries in the microstructure 1B, giving rise to the network

of the white regions in Fig. 5(d). Second, there is some decomposition of the aligned laths of the 1B structure.

The interpretation of these features seems straightforward. On heating, the high nickel laths should revert to γ, giving rise to the first peak in the dilatometer trace in Fig. 4(b). At slightly higher temperature the low Ni matrix will begin to transform, causing the discontinuity in the slope of the dilatometer trace in Fig. 4(b). At 730°C the initial microstructure should consist of a mixture of high-nickel and lower nickel γ, with a possible admixture of retained α in the low nickel regions. This structure is unstable because of the heterogenous nickel concentration and will tend to homogenize. It cannot homogenize by simple diffusion because of the low bulk diffusivity of Ni in γ iron at this temperature and concentration[11] (the mean diffusion distance for Ni in γ, $(2Dt)^{1/2}$, is $\sim$0.05 μm after two hours at 730°C). However, nucleated homogeneous γ can grow perpendicular to the platelet planes through interface diffusion of nickel. Interface diffusion can also cause some decomposition of the individual platelets; however the bulk of the material within grains retains an oriented platelet morphology.

The oriented substructure of the alloy is broken up during the next two-phase decomposition, cycle 2B. The resulting microstructure is shown in Fig. 5(e) and in Fig. 6(e) and (f). Platelet orientation within grains is largely destroyed by the nucleation and growth transformation, and an ultrafine grained microstructure results. The network of homogenized material in the 2A microstructure also decomposes on a finer scale. The resulting grain size (0.5-2.0 μm; ASTM #15-#18) is considerably below the

best we have been able to obtain with simple cyclic austenitizing treatments and is comparable to that Miller[7] obtained after severe cold working.

The grain-refined alloy is apparently completely ferritic. No retained austenite was detected using conventional x-ray techniques. R. L. Miller[12] confirmed this result using a modification of his reported techniques[13, 14] which permits detection of as little as 0.1% retained austenite.

We have explored the effect of adding additional 730°C/650°C cycles. These do give an apparent additional refinement of the larger grains remaining in the microstructure, but the effect is small and has no obvious influence on cryogenic mechanical properties.

III. MECHANICAL PROPERTIES AT CRYOGENIC TEMPERATURES

The mechanical test specimens were taken from the material prepared as described in section II(a). The annealed 0.75" (1.9 cm) thick plates were cut into pieces 2.75" (7.0 cm) long. These pieces were then given selected thermal processing. After processing, one fracture toughness specimen and two Charpy impact specimens were machined from each piece along the longitudinal direction of forging, ensuring the same heat treatment for both tests. Tensile specimens (transverse direction) were obtained from the far end of the broken fracture toughness specimens.

(a) Cryogenic Tensile Properties

Tensile tests were conducted at liquid nitrogen temperature using an Instron machine equipped with a cryostat. Subsize specimens of 0.5" (1.27 cm) gauge length and 0.125" (0.32 cm) diameter were tested at a crosshead speed of 0.02 in./minute (0.05 cm/minute). Two specimens were

tested at each stage of the cycling treatment. The deviation in yield strength between tests was $\sim$5 ksi (35 newton/m^2).

The results of the tensile tests are shown in Table I. The yield strength at 77°K is in the range 140-150 ksi (9.66-10.35 x 10^8 newton/m^2) and is rather insensitive to microstructure. The samples treated to stages 1B and 2B have slightly higher yield strength and lower tensile ductility than those at states 1A and 2A. These minor effects appear to be due to the precipitation of Ni_3Ti in the α phase at 650°C. Electron microscopic studies indicate that the extent of this precipitation is small.

(b) Cryogenic Impact Properties

Charpy V-notch impact tests were conducted at liquid nitrogen temperature (77°K) using ASTM standard techniques[15], and near liquid helium temperature (5-6°K), using a method recently developed in this laboratory[16]. Two specimens were tested at each condition. The results of these tests are presented in Table II. The broken specimens are shown in Fig. 7.

At 77°K all four structures showed high toughness. However, at 6°K specimens 1A and 1B were brittle. Fractographs taken at the center of the fracture surface in these specimens revealed a quasi-cleavage fracture mode. Specimens 2A and 2B remained tough at 6°K; the transition temperatures in charpy testing for the bcc structures 2A and 2B are below this temperature.

(c) Cryogenic Fracture Toughness

Fracture toughness tests were conducted at 77°K on an MTS machine equipped with a liquid nitrogen cryostat. Compact tension (WOL) specimens

of 0.70" (1.78 cm) thickness were prepared and fatique precracked according to ASTM specifications[17]. Two specimens were tested at each stage of the thermal cycling treatment.

The results of these tests are shown in Fig. 8. With the possible exception of sample 1B, these specimens were well away from plane strain conditions; a value of $K_Q \sim 140$ KSI$\cdot\sqrt{in}$ was computed from the load-crack opening displacement (COD) curves[17]. At stages 1A, 1B, and 2A the alloy exhibited unstable crack propagation as marked by the dotted lines in the load -COD curves. However the fine-grained alloy 2B seemed immune to unstable crack propagation. The specimen was fully plastic, and the pre-induced crack grew slowly in a stable manner until the test was stopped. The post-test fracture toughness specimens are compared to one another in Fig. 9. The brittleness of specimens 1A and 1B, the repeated crack arrest in specimen 2A, and the ductility of specimen 2B are visually apparent.

The fracture surfaces were examined by scanning electron microscopy. Fig. 10 shows scanning electron fractographs taken slightly ahead of the pre-induced fatigue crack along the center line of the sample. Specimens processed to stages 1A and 1B propagated fracture in a quasi-cleavage mode. At stage 2A, the fracture mode was a mixture of quasi-cleavage and ductile rupture. Fully grain refined specimens (2B) showed ductile dimple rupture over the whole fracture surface.

CONCLUSIONS

(1) By alternate phase transformation in γ and $(\alpha + \gamma)$ range, the grain size of an Fe-12Ni-0.25Ti alloy was refined from 40~60 μm to 0.5~2 μm in 4 cycles.

(2) With this ultrafine grain size, the ductile brittle transition temperature of this ferritic alloy in Charpy impact testing was suppressed below liquid helium temperature.

(3) The ductile-brittle transition temperature in a fracture toughness testing with a sharp crack was suppressed below liquid nitrogen temperature and the fracture mode was changed from brittle quasi-cleavage to completely ductile dimple rupture.

ACKNOWLEDGEMENTS

The authors wish to thank Dr. R. L. Miller of the U. S. Steel Corporation for assistance in retained austenite analysis. They are also grateful to Professor R. M. Fulrath for assistance with the dilatometric and x-ray analyses, and to Professor G. Thomas for helpful discussions.

The work reported here was supported by the Office of Naval Research under contract N00014-69-A-1062, NR031-762, and by the Atomic Energy Commission through the Inorganic Materials Research Division of the Lawrence Berkeley Laboratory.

REFERENCES

1. W. A. Horwood: M. S. Thesis, University of California Berkeley, 1972
2. S. Jin, J. W. Morris, Jr. and V. F. Zackay: Advances in Cryogenic Engineering, Vol. 19, 1974, in press.
3. G. Sasaki: Ph.D Thesis, University of California, Berkeley, 1973.
4. V. F. Zackay: Proceedings of the Third International Conference on the Strength of Metals and Alloys, Vo. 1, August, 1973, p. 591.
5. L. F. Porter and D. S. Dabkowski: Ultrafine Grain Metals, 1972, Syracuse University Press, p. 113.
6. G. Saul, J. A. Roberson, and A. M. Adair: Met. Trans., 1970, Vol. 1, p. 383.
7. R. L. Miller: Met. Trans., 1972, Vol. 2, p. 905.
8. R. A. Grange: Trans. ASM, 1966, Vol. 59, p. 26.
9. S. Floreen: Met. Rev., 1968, p. 115.
10. M. Hansen: Constitution of Binary Alloys, 2nd Ed., McGraw-Hill, New York, 1958, p. 677.
11. C. F. Hancock and G. M. Leak: Metal Sci. J., 1967, Vol. 1, p.33.
12. R. L. Miller: Research Lab. of U. S. Steel Corp., Monroeville, Pennsylvania, Private Communication.
13. R. L. Miller: Trans. ASM., 1964, Vol. 57, p. 892.
14. R. L. Miller: Trans. ASM., 1968, Vol. 61, p. 592.
15. 1973 Book of ASTM Standard, part 31, E 23-72, p. 277.
16. S. Jin, W. A. Horwood, J. W. Morris, Jr. and V. F. Zackay: Advances in Cryogenic Engineering, Vol. 19, 1974, in press.
17. 1973 Book of ASTM Standards, part 31, E 399-72, p. 960.

Table I. Results of the Tensile Tests at $77^{o}K$

Specimen	Yield Strength ksi (newton/m^2)	Tensile Strength ksi (newton/m^2)	Elong. %	R. A. %
1A	134 (9.25×10^8)	142 (9.80×10^8)	31.1	73.8
1B	145 (10.09×10^8)	151 (10.42×10^8)	24.8	70.5
2A	141 (9.73×10^8)	150 (10.35×10^8)	29.3	72.9
2B	149 (10.28×10^8)	154 (10.63×10^8)	26.8	72.1

Table II. Charpy Impact Energy at $77^{o}K$ and $6^{o}K$

Specimen	Impact Energy at $77^{o}K$ ft-lb (newton-meter)	Impact Energy at $6^{o}k$ ft-lb (newton-meter)
1A	154 (209)	55 (75)
1B	116 (158)	43 (59)
2A	131 (178)	116 (158)
2B	115 (156)	99 (134)

FIGURE CAPTIONS

Fig. 1 - The Fe-Ni equilibrium phase diagram with heat treating cycles.

Fig. 2 - Dilatometric analysis of the phase transformations in Fe-12Ni-0.25Ti alloy, (a) on continuous heating and cooling, (b) on isothermal decomposition with the ($\alpha + \gamma$) range for different periods.

Fig. 3 - Estimated isothermal transformation rate at 650°C.

Fig. 4 - (a) Dilatometry for an initially homogeneous specimen (same as Fig. 2(a)), (b) dilatometry for a specimen initially decomposed at 650°C for 2 hours. After the transformation of the duplex structure to γ is finished, the specimen was held at 730°C for two hours for partial homogenization and then cooled to room temperature, (c) same as (b) except that the homogenization was minimized by holding at 730°C for just a few seconds. (d) The homogenization cycle (b) was followed by another continuous heating to the γ range to see the change in A_s, A_f temperatures from those of (a) and (b).

Fig. 5 - Change of optical microstructures on thermal cyclings. (a) starting microstructure (900°C 2 hours annealed), (b) after cycle 1A, (c) after cycle 1B, (d) after cycle 2A, (e) after cycle 2B (final microstructure).

Fig. 6 - Scanning electron microstructures. (a), (b) specimen 1B. (C) (d) specimen 2A, (e) (f) specimen 2B. The micrographs (b), (d) and (f) are of higher magnification.

Fig. 7 - Photographs of the broken Charpy bars after testing at 77°K and 6°K.

Fig. 8 — Load-crack opening displacement curves in fracture toughness testing at $77^{\circ}K$.

Fig. 9 — Post-test fracture toughness specimens.

Fig. 10 — Scanning electron microscope fractographs of the specimens shown in Fig. 9.

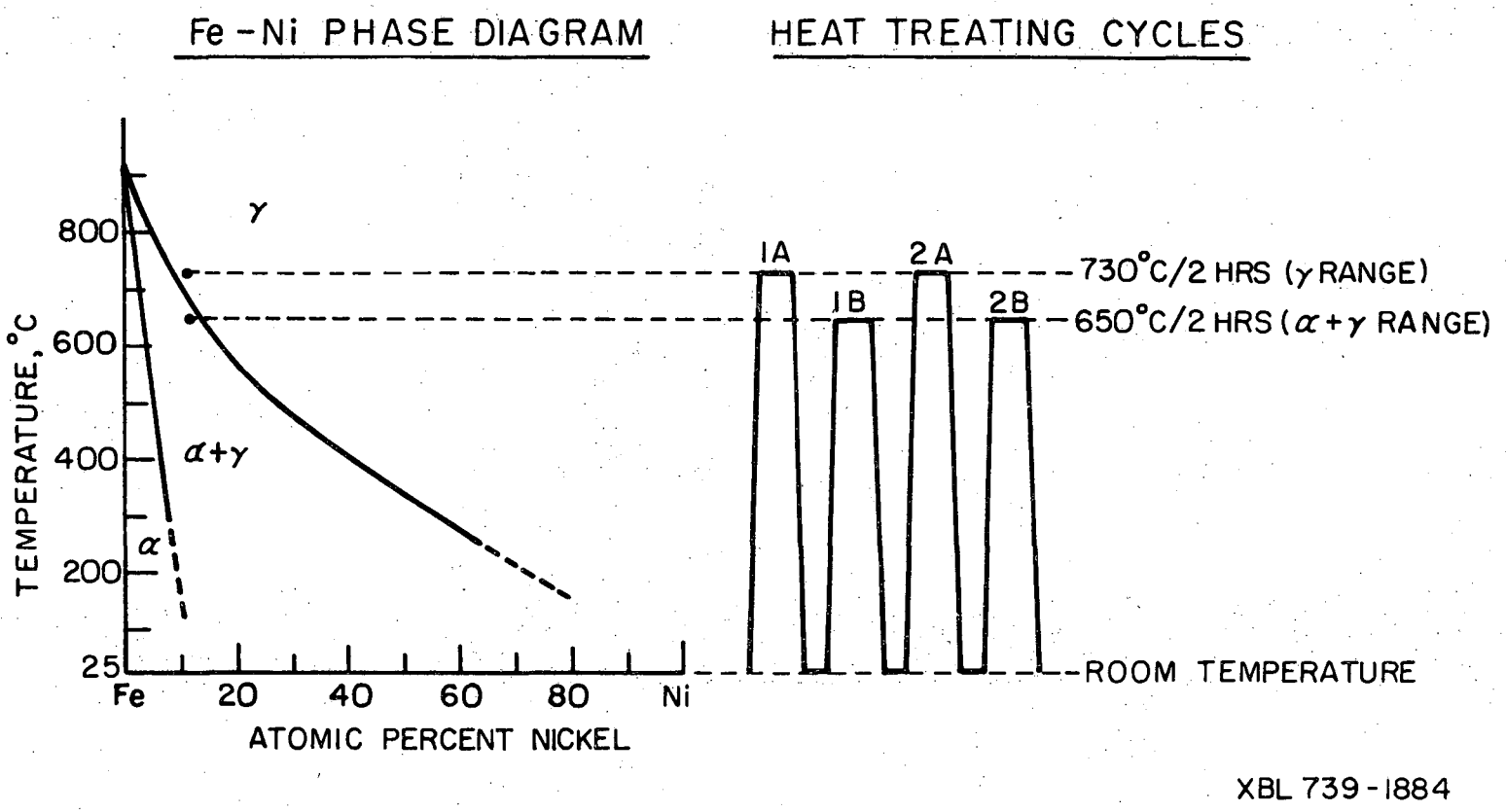
Fe - Ni PHASE DIAGRAM
HEAT TREATING CYCLES
TEMPERATURE, °C
800
600
400
200
25
γ
α+γ
α
Fe
20
40
60
80
Ni
ATOMIC PERCENT NICKEL
1A
2A
1B
2B
730°C/2 HRS (γ RANGE)
650°C/2 HRS (α+γ RANGE)
ROOM TEMPERATURE
XBL 739-1884

Fig. 1

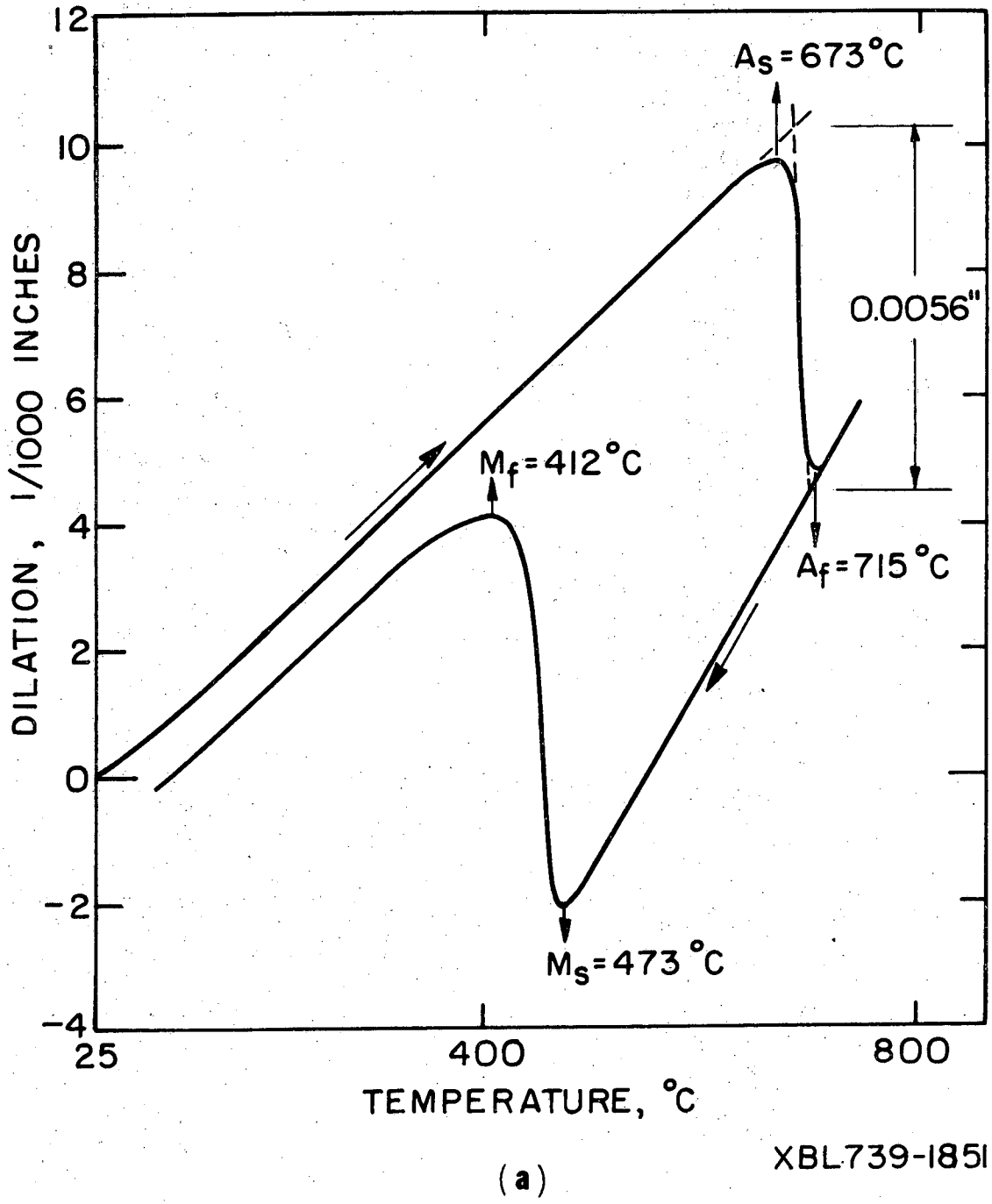
12
10
8
6
4
2
0
-2
-4
DILATION, 1/1000 INCHES
25
400
800
TEMPERATURE, °C
A_s = 673°C
M_f = 412°C
A_f = 715°C
M_s = 473°C
0.0056"
XBL739-1851

(a)

Fig. 2

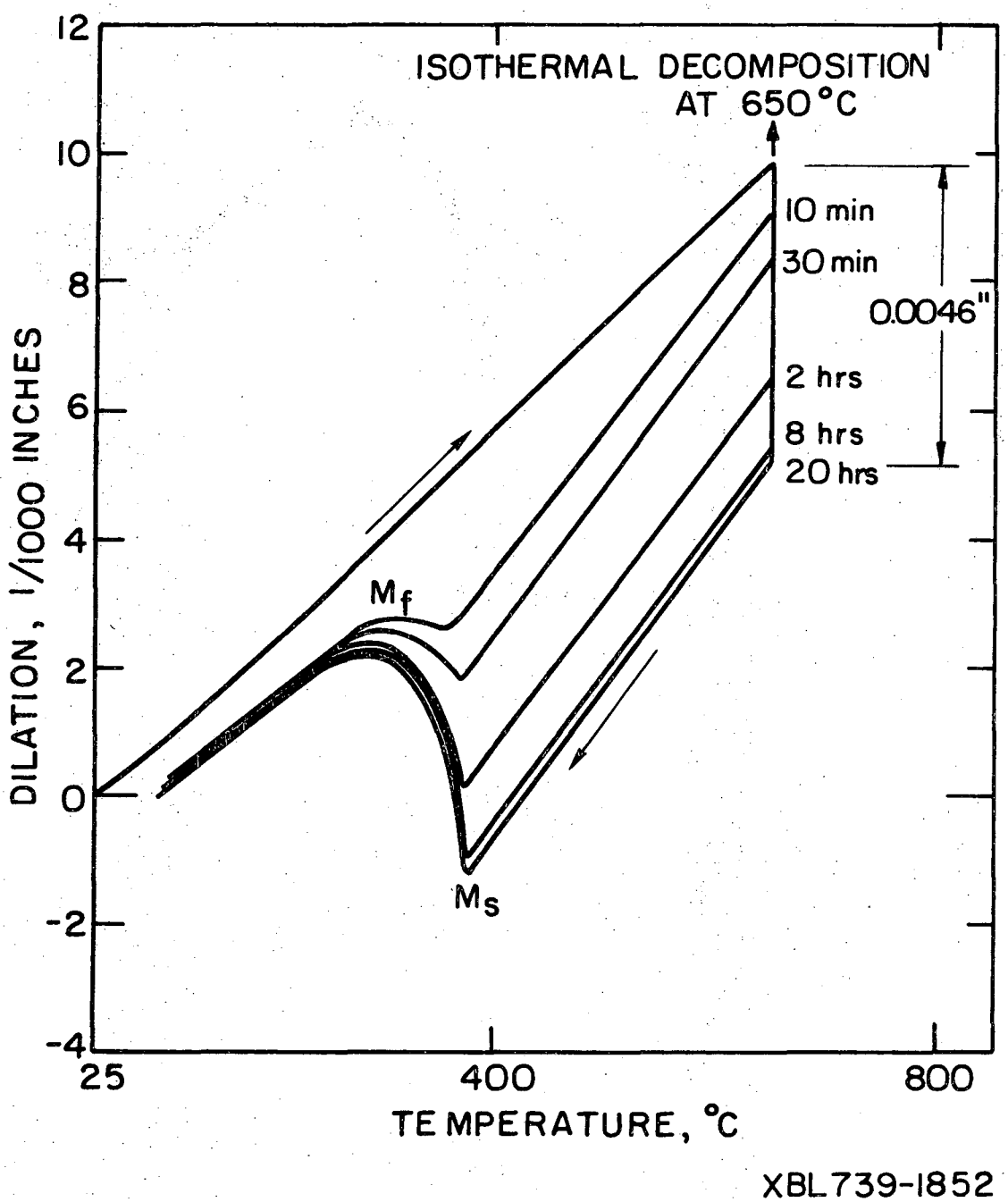
ISOTHERMAL DECOMPOSITION
AT 650°C
10 min
30 min
0.0046"
2 hrs
8 hrs
20 hrs
M_f
M_s
DILATION, 1/1000 INCHES
TEMPERATURE, °C
12
10
8
6
4
2
0
-2
-4
25
400
800
XBL739-1852

(b)

Fig. 2 (cont.)

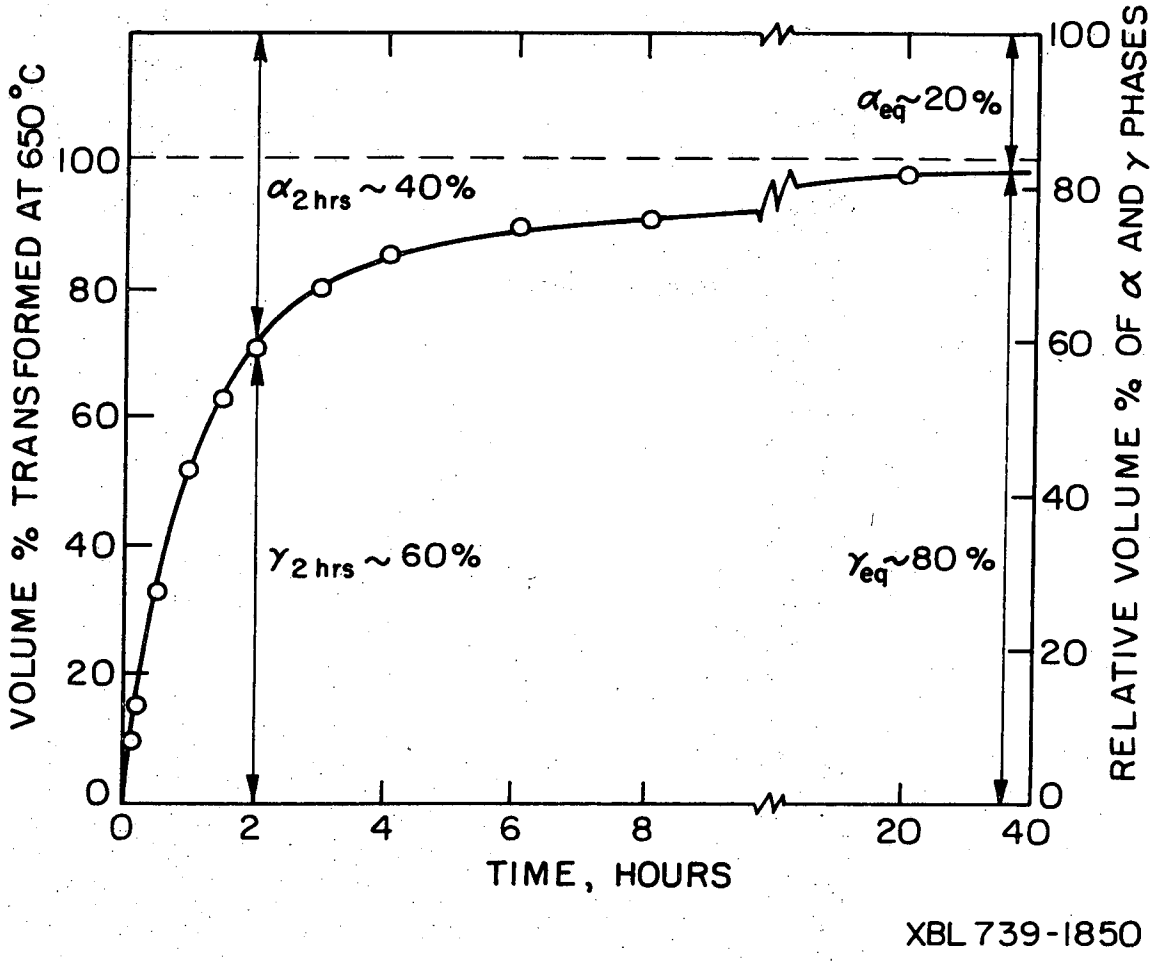
VOLUME % TRANSFORMED AT 650°C
RELATIVE VOLUME % OF α AND γ PHASES
TIME, HOURS
$\alpha_{2\,hrs} \sim 40\%$
$\gamma_{2\,hrs} \sim 60\%$
$\alpha_{eq} \sim 20\%$
$\gamma_{eq} \sim 80\%$
0
20
40
60
80
100
0
2
4
6
8
20
40
XBL 739-1850

Fig. 3

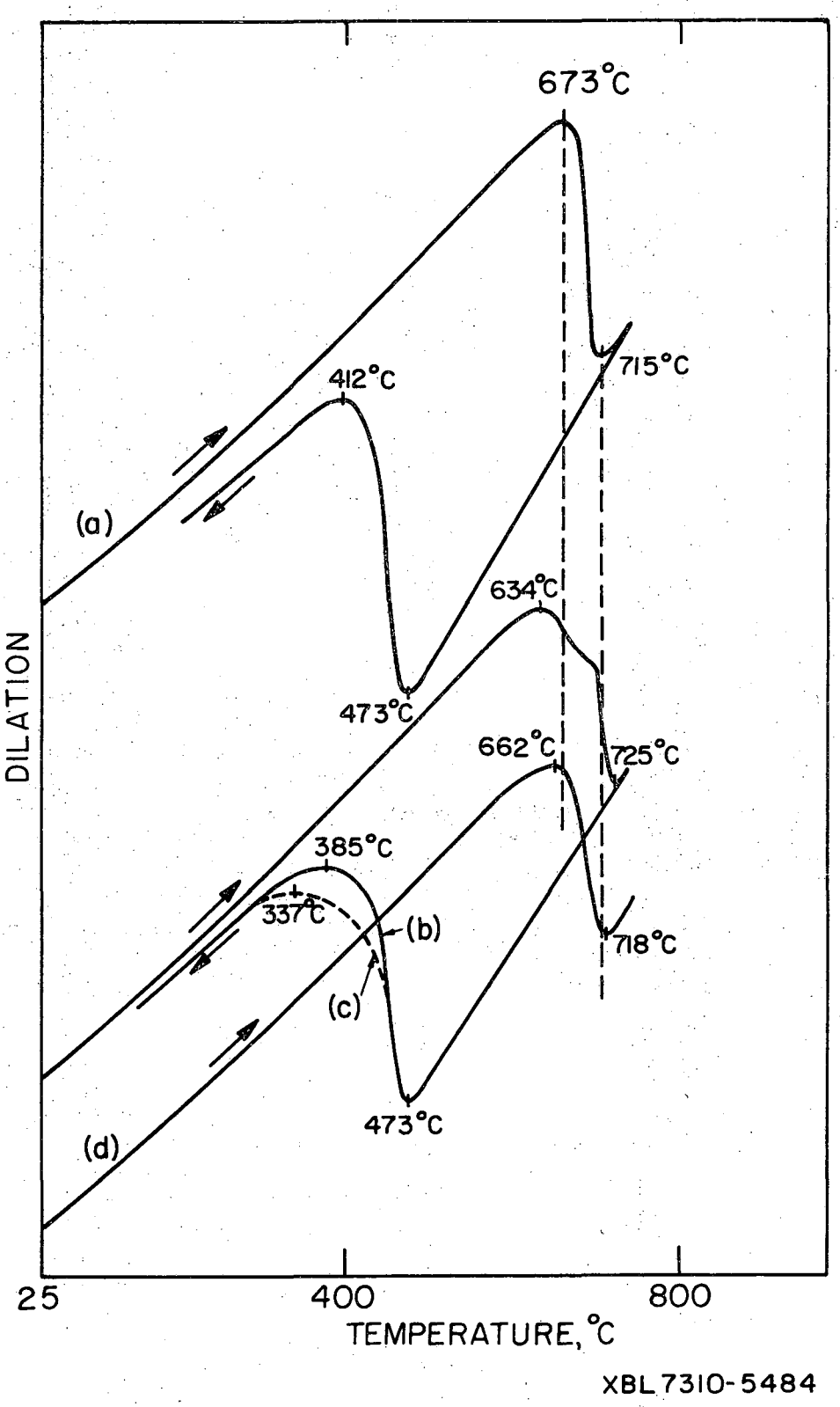
673°C
412°C
715°C
(a)
634°C
473°C
662°C
725°C
385°C
337°C
(b)
718°C
(c)
473°C
(d)
DILATION
25
400
800
TEMPERATURE, °C
XBL 7310-5484

Fig. 4

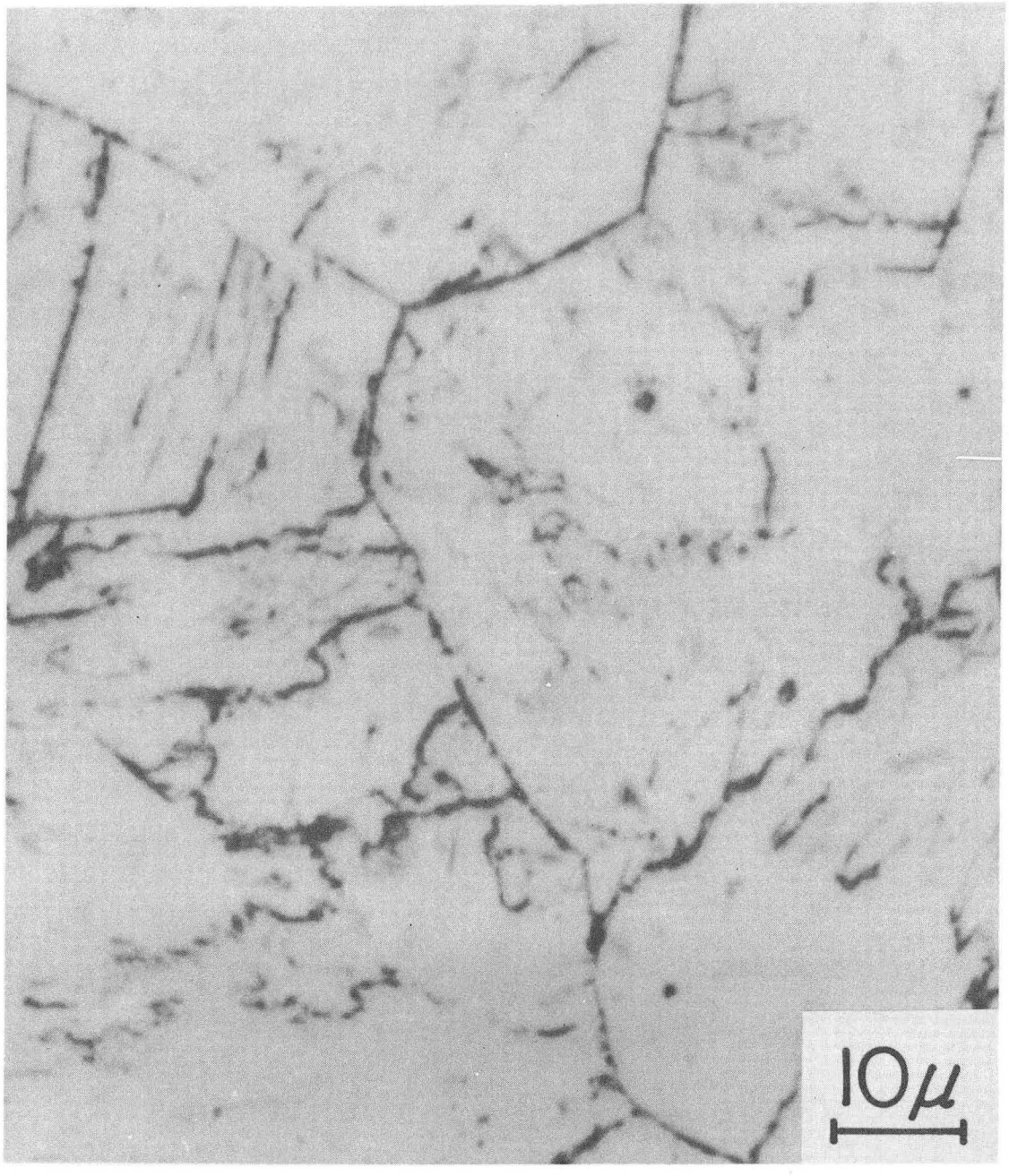

XBB 739-5688

Fig. 5(a)

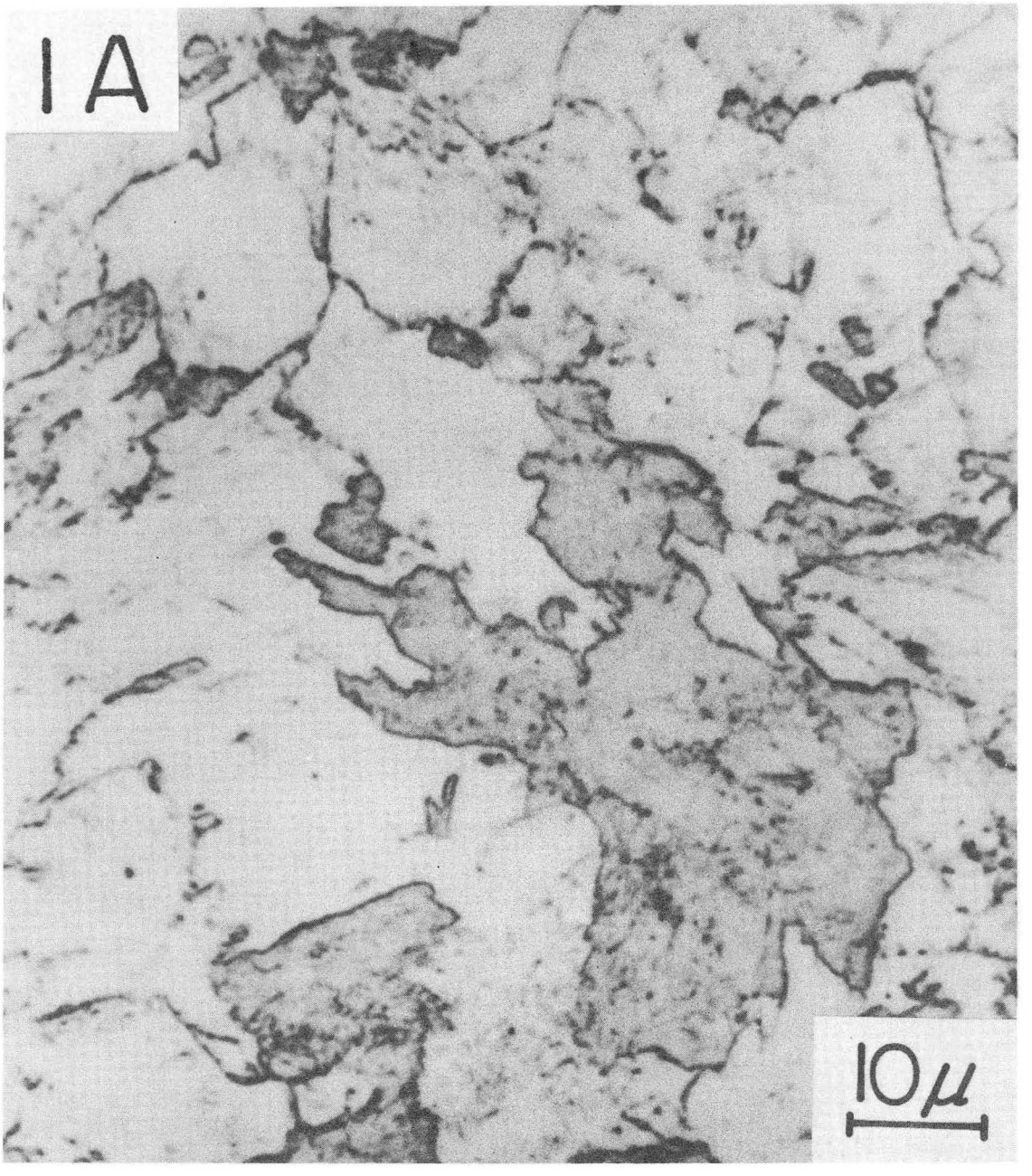

XBB 739-5689

Fig. 5(b)

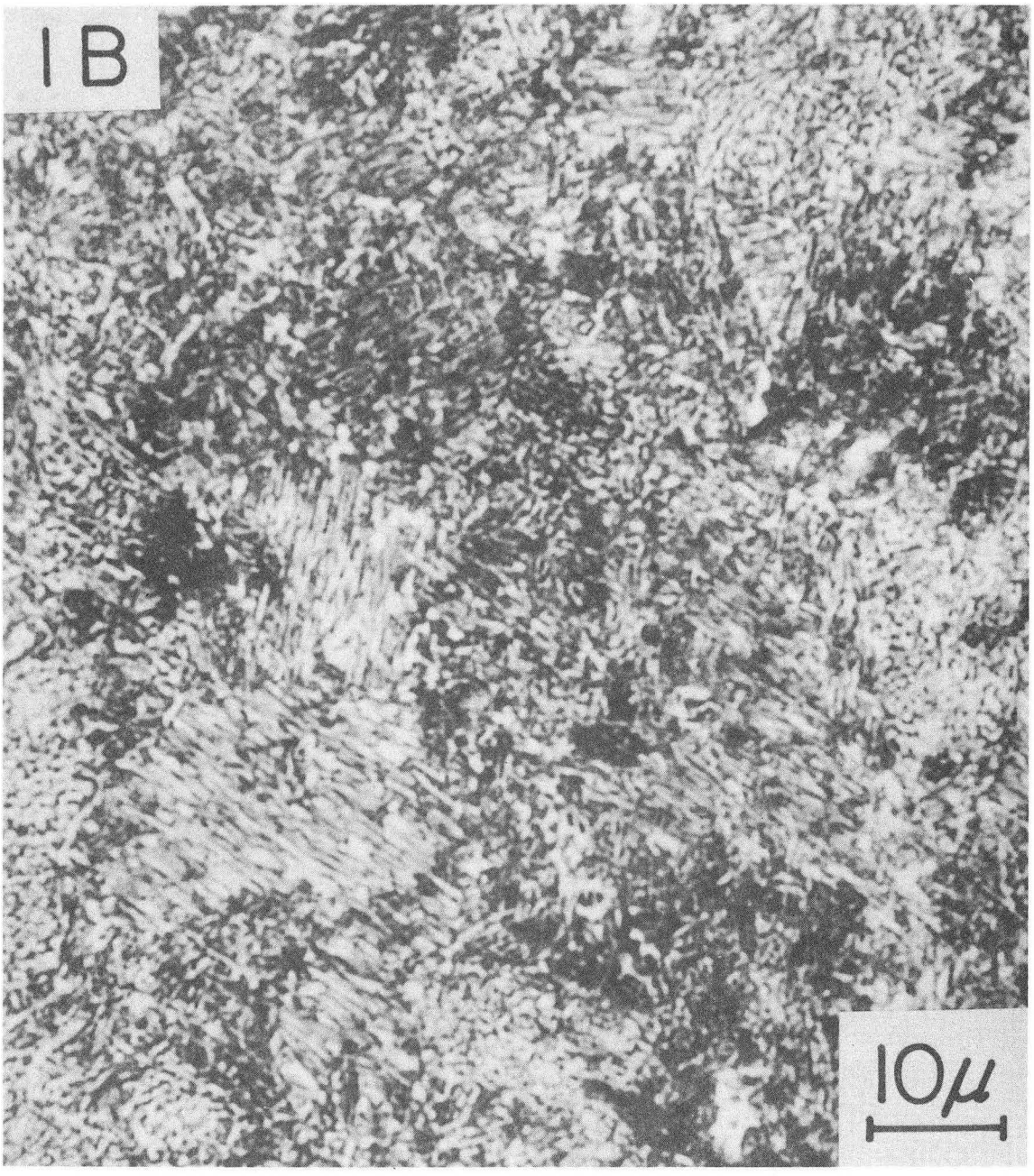

XBB 739-5690

Fig. 5(c)

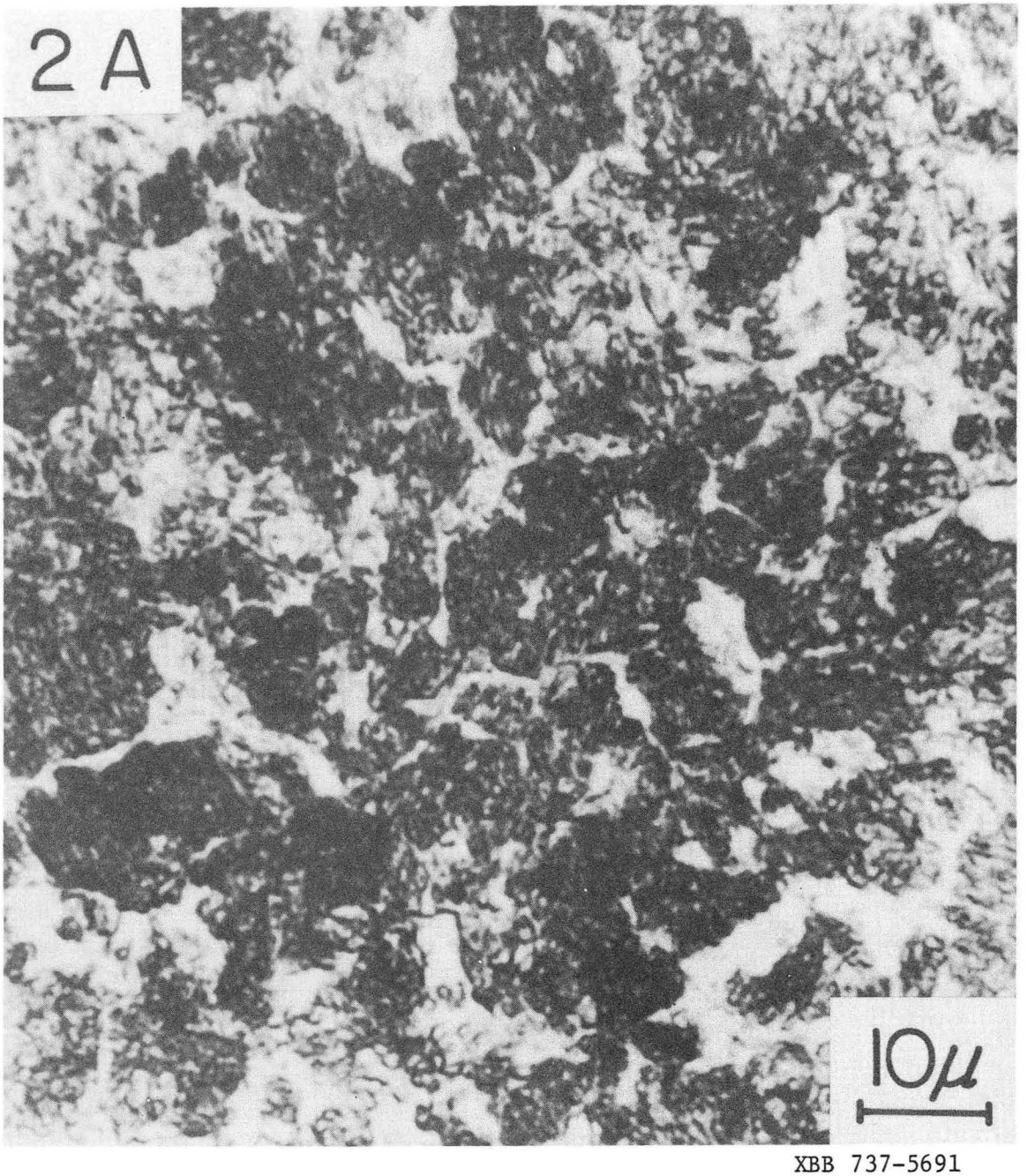

XBB 737-5691

Fig. 5(d)

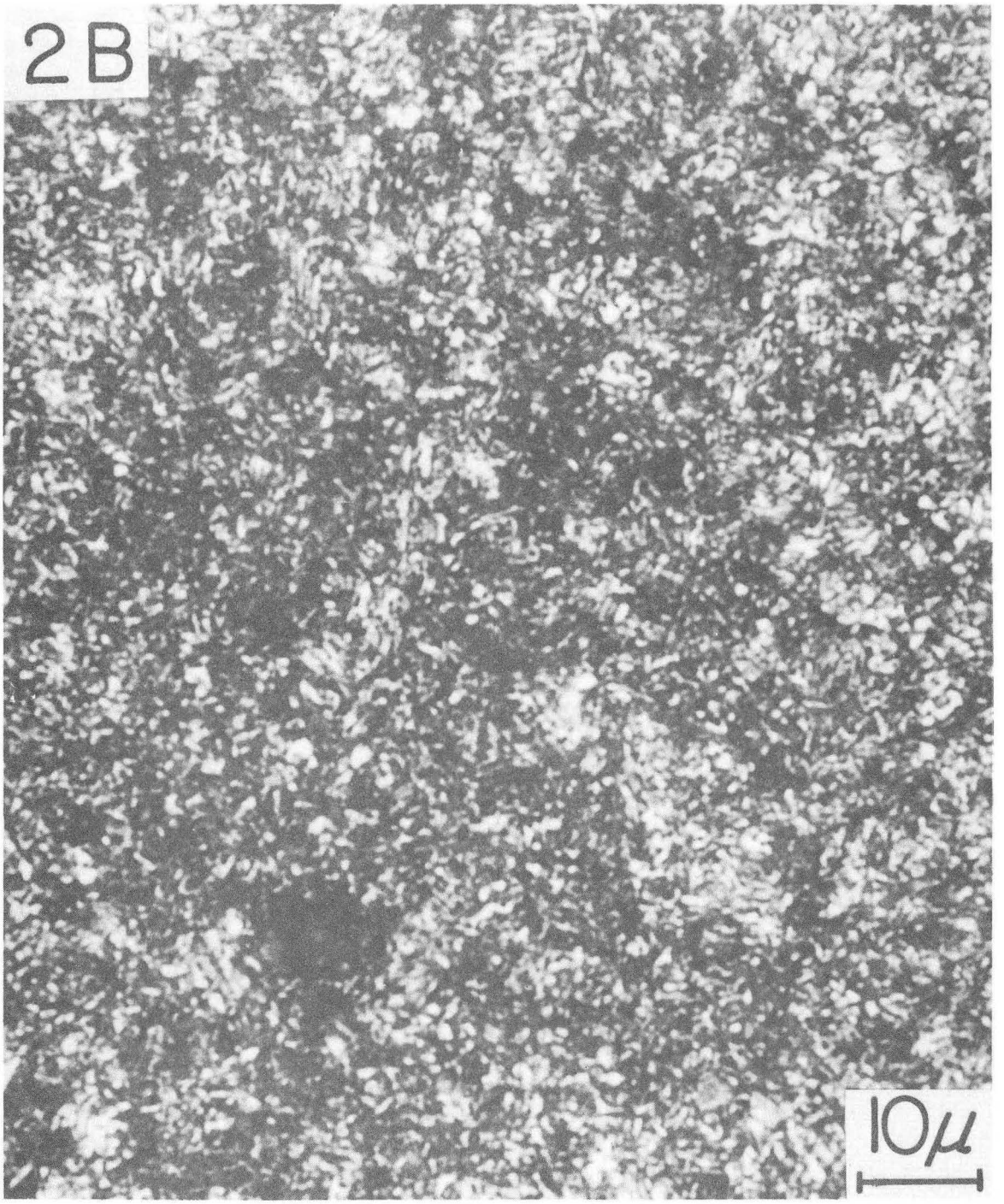

XBB 7312-7363

Fig. 5(e)

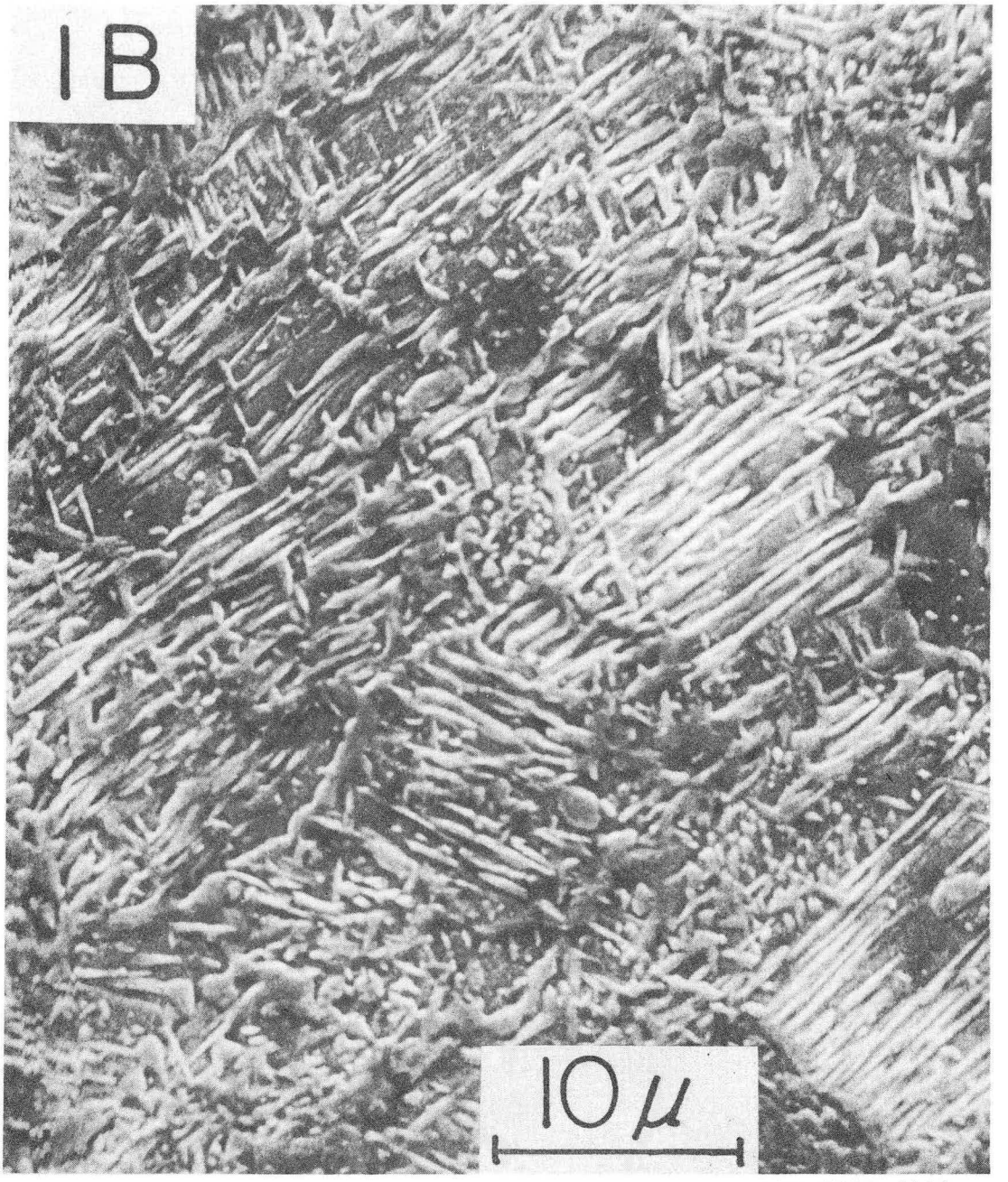

XBB 7310-6446

Fig. 6(a)

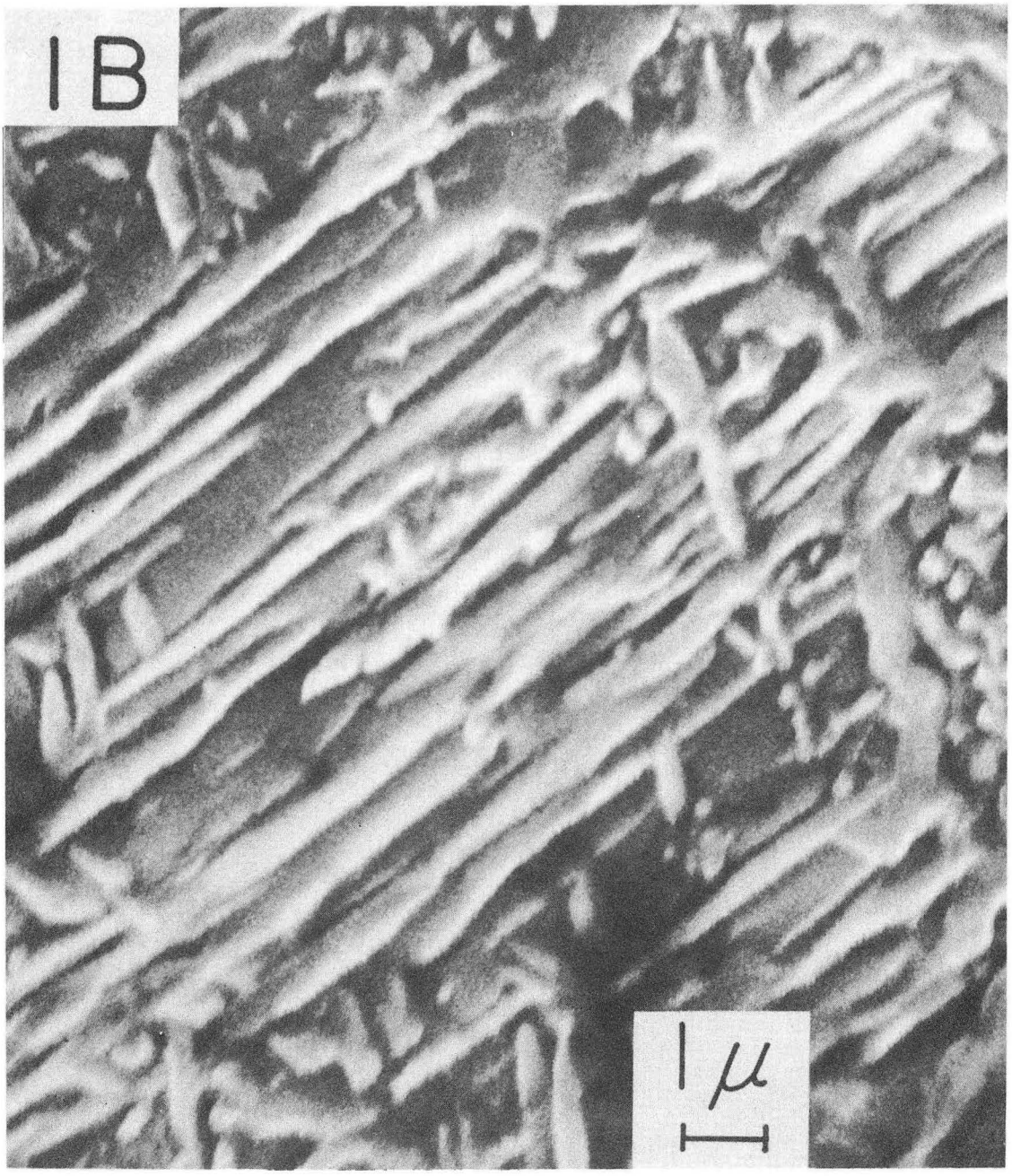

XBB 7310-6445

Fig. 6(b)

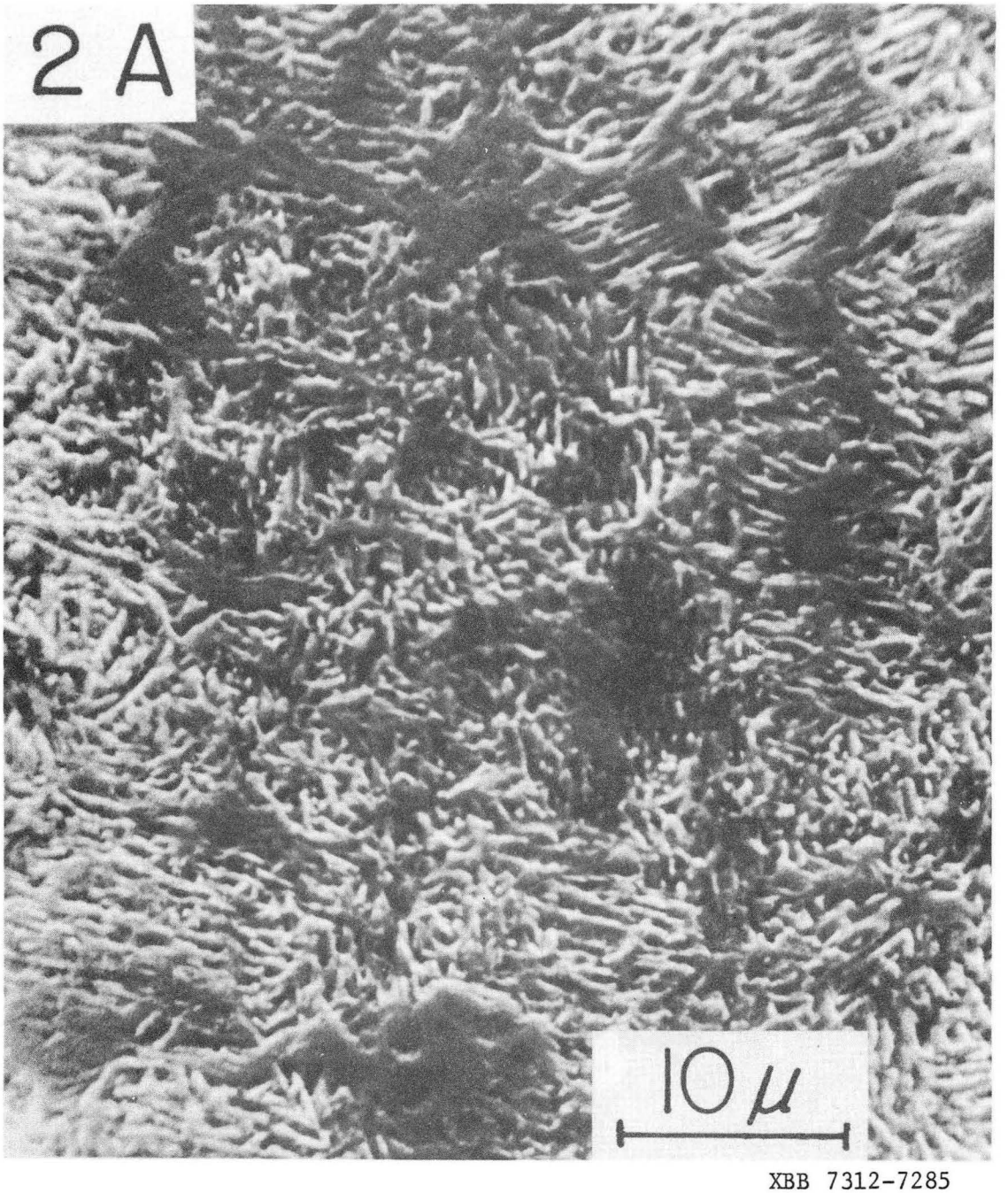

XBB 7312-7285

Fig. 6(c)

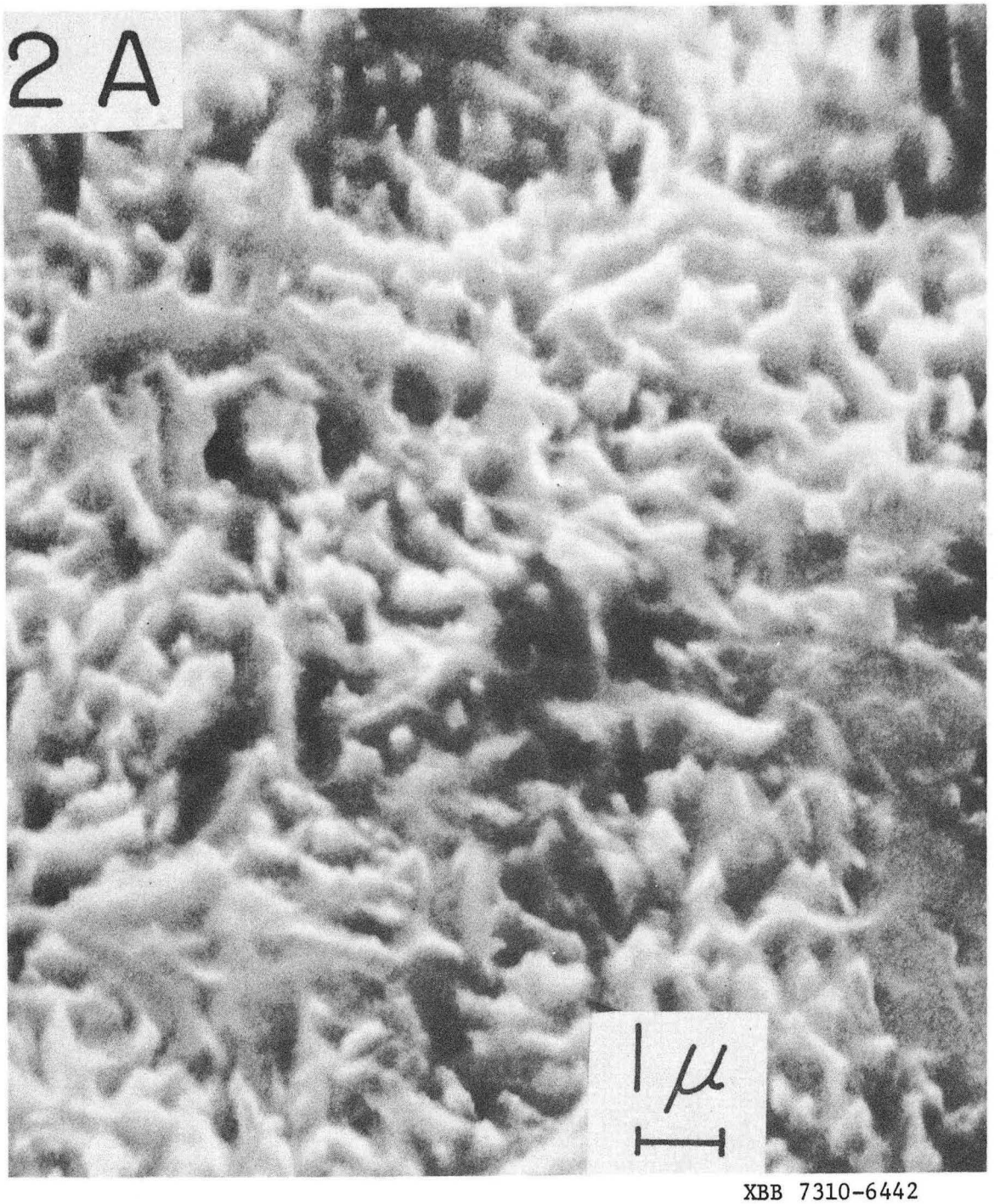

XBB 7310-6442

Fig. 6(d)

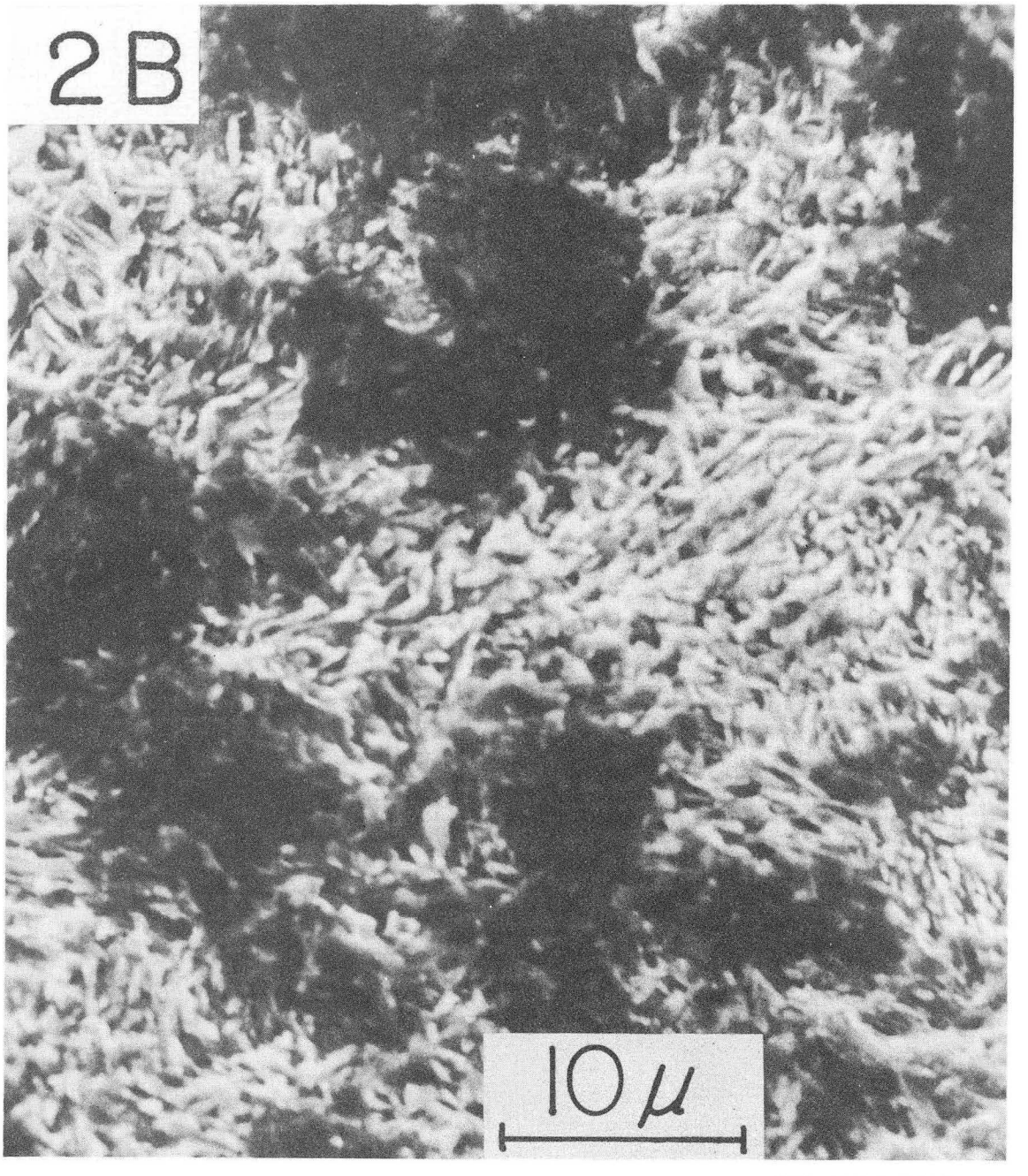

XBB 7310-6441

Fig. 6(e)

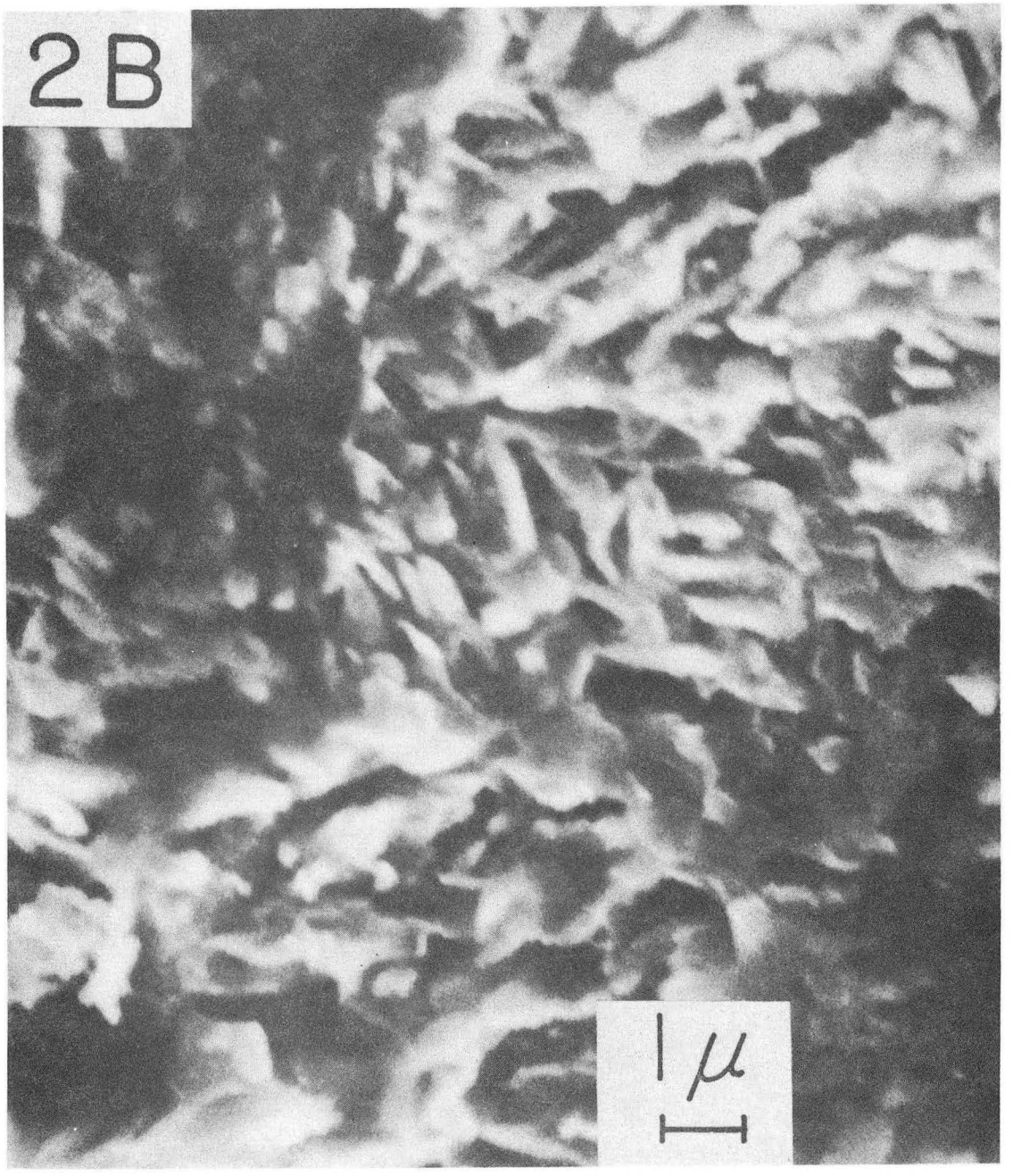

XBB 7310-6444

Fig. 6(f)

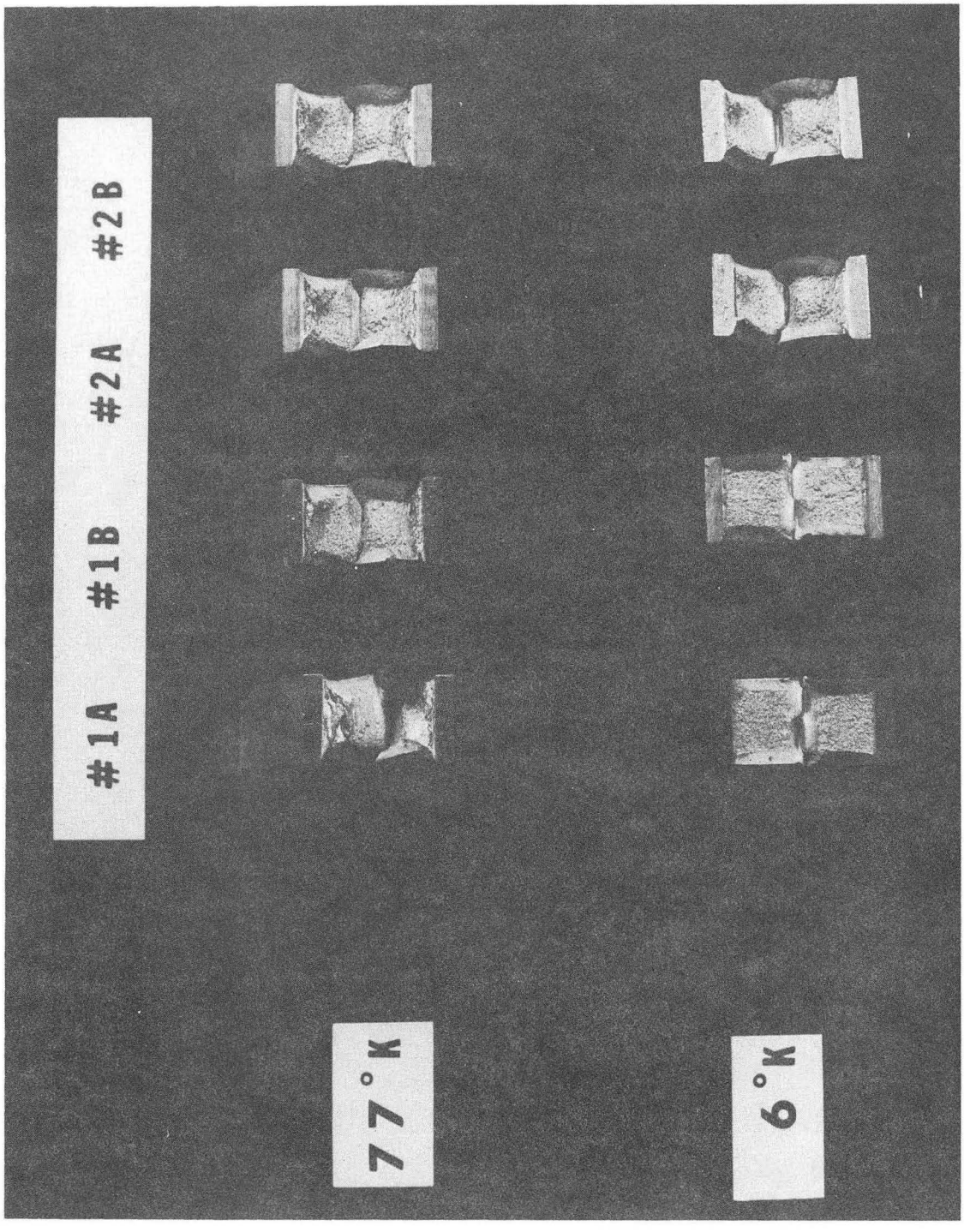

XBB 739-5645

Fig. 7

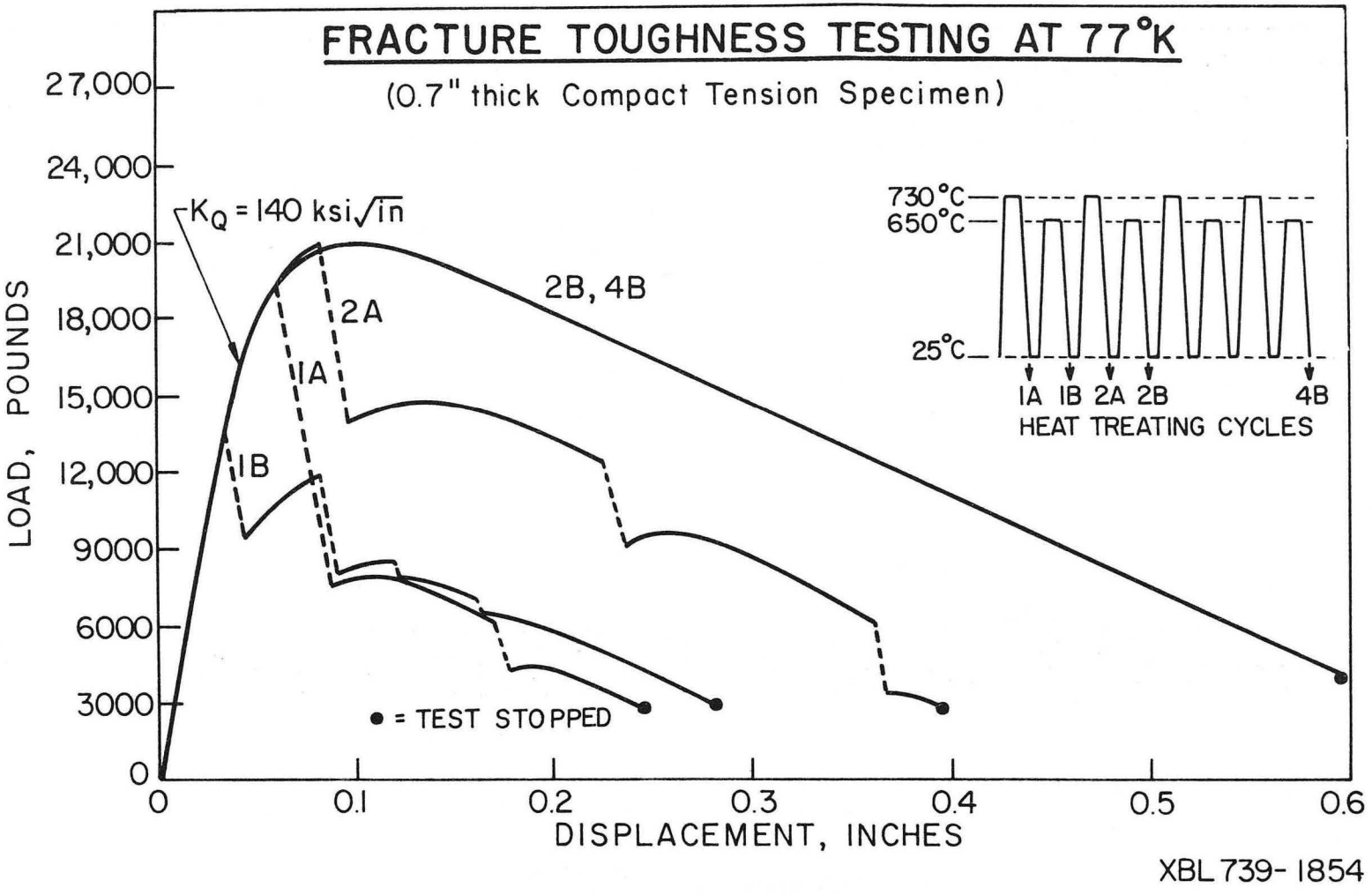
FRACTURE TOUGHNESS TESTING AT 77°K
(0.7" thick Compact Tension Specimen)
LOAD, POUNDS
27,000
24,000
21,000
18,000
15,000
12,000
9000
6000
3000
0
K_Q = 140 ksi$\sqrt{in}$
2B, 4B
2A
1A
1B
● = TEST STOPPED
730°C
650°C
25°C
1A 1B 2A 2B 4B
HEAT TREATING CYCLES
0
0.1
0.2
0.3
0.4
0.5
0.6
DISPLACEMENT, INCHES
XBL 739-1854

Fig. 8

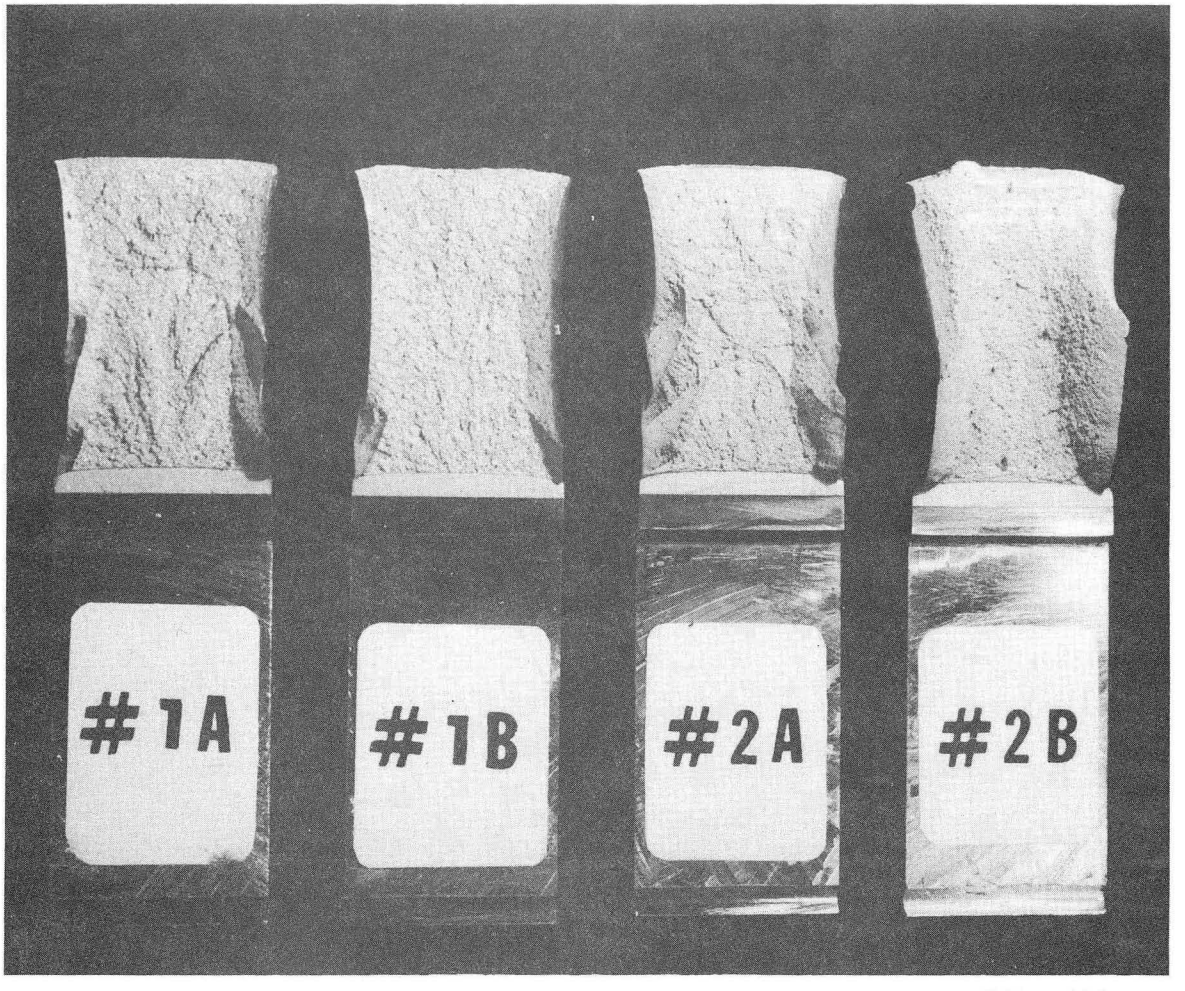

XBB 739-5644

Fig. 9

FRACTOGRAPHS

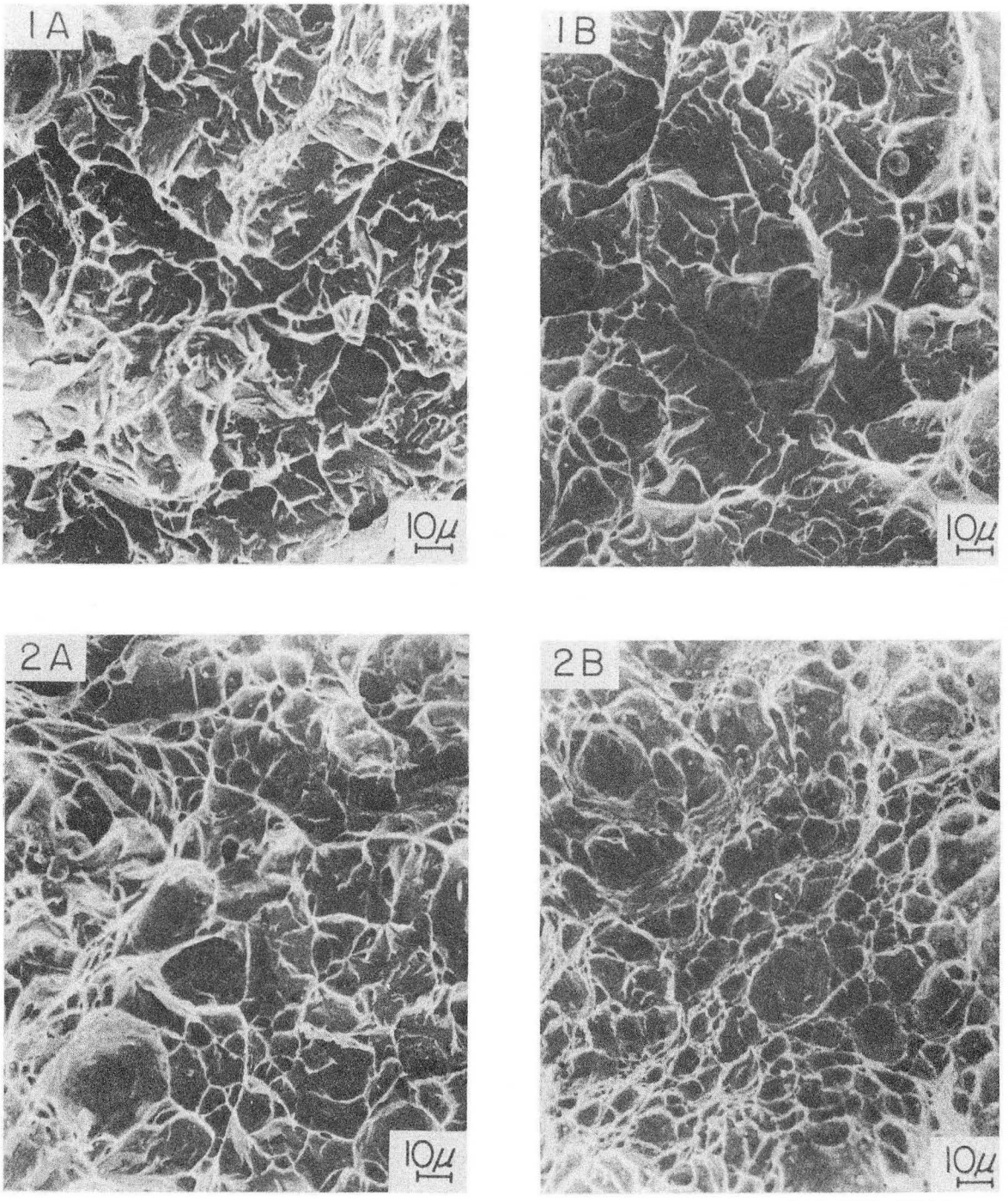

XBB 739-5678

Fig. 10

TECHNICAL INFORMATION DIVISION
LAWRENCE BERKELEY LABORATORY
UNIVERSITY OF CALIFORNIA
BERKELEY, CALIFORNIA 94720